Supplementary Material: Appendices to Bayesian Analysis of Latent Threshold Dynamic Models

Jouchi Nakajima & Mike West

Journal of Business & Economic Statistics, 31(2):151–164, 2013

DOI: 10.1080/07350015.2012.747847

A Posterior computation and MCMC algorithm

A.1 LT regression model

In the LT regression model defined by eqns. (1)-(3), we describe a MCMC algorithm for simulation of the full joint posterior $p(\mathbf{\Theta}, \sigma, \boldsymbol{\beta}_{1:T}, \boldsymbol{d}|\boldsymbol{y}_{1:T})$. We assume prior forms of the following: $\mu_i \sim N(\mu_{i0}, w_{i0}^2)$, $(\phi_i+1)/2 \sim \pi(\phi_i)$, $\sigma_{i\eta}^{-2} \sim G(v_{0i}/2, V_{0i}/2)$, $\sigma^{-2} \sim G(n_0/2, S_0/2)$, $\beta_{i1}|\Theta \sim N(\mu_i, v_i^2)$, and $d_i \sim U(0, |\mu_i| + K_i v_i)$.

A.1.1 Sampling $\mathbf{\Theta}$ and σ

Conditional on $(\boldsymbol{\beta}_{1:T}, \boldsymbol{d}, \boldsymbol{y}_{1:T})$, sampling of the VAR parameters $\mathbf{\Theta}$ reduces to generation from conditionally independent posterior $p(\boldsymbol{\theta}_i|\beta_{i,1:T}, d_i)$, for $i = 1:k$. First, the conditional posterior density of μ_i is

$$p(\mu_i|\phi_i, \sigma_{i\eta}, \beta_{i,1:T}, d_i) \propto TN_{D_i}(\mu_i|\hat{\mu}_i, \hat{w}_i^2)(|\mu_i| + Kv_i)^{-1},$$

where TN_{D_i} denotes the density of a truncated normal for μ_i on $D_i = \{\mu_i : d_i < |\mu_i| + K_i v_i\}$, and

$$\begin{aligned} \hat{w}_i^2 &= \left\{ \frac{1}{w_{i0}^2} + \frac{(1-\phi_i^2) + (T-1)(1-\phi_i)^2}{\sigma_{i\eta}^2} \right\}^{-1}, \\ \hat{\mu}_i &= \hat{w}_i^2 \left\{ \frac{\mu_{i0}}{w_{i0}^2} + \frac{(1-\phi_i^2)\beta_{i1} + (1-\phi_i)\sum_{t=1}^{T-1}(\beta_{i,t+1} - \phi_i \beta_{it})}{\sigma_{i\eta}^2} \right\}. \end{aligned}$$

A Metropolis-Hastings step draws a candidate μ_i^* from this truncated normal, accepting the draw with probability

$$\min\left\{1,\ \frac{|\mu_i| + Kv_i}{|\mu_i^*| + Kv_i}\right\}.$$

Second, the conditional posterior density of ϕ_i is

$$p(\phi_i|\mu_i, \sigma_{i\eta}, \beta_{i,1:T}, d_i) \propto \pi(\phi_i)(1-\phi_i^2)^{1/2} TN_{(-1,1)\times E_i}(\hat{\phi}_i, \sigma^2_{\phi_i})\{|\mu_i| + K_i\sigma_{i\eta}/(1-\phi_i^2)^{1/2}\}^{-1},$$

where $\hat{\phi}_i = \sum_{t=1}^{T-1} \bar{\beta}_{i,t+1}\bar{\beta}_{it} / \sum_{t=2}^{T-1} \bar{\beta}_{it}^2$, $\sigma^2_{\phi_i} = \sigma^2_{i\eta} / \sum_{t=2}^{T-1} \bar{\beta}^2_{it}$ with $\bar{\beta}_{it} = \beta_{it} - \mu_i$, and E_i is the truncation region $E_i = \{\phi_i : d_i < |\mu_i| + K_i\sigma_{i\eta}/(1-\phi_i^2)^{1/2}\}$. A Metropolis-Hastings step draws a candidate ϕ_i^* from this truncated normal, accepting the draw with probability

$$\min\left\{1, \frac{\pi(\phi_i^*)(1-\phi_i^{*2})^{1/2}\{|\mu_i| + K_i\sigma_{i\eta}/(1-\phi_i^2)^{1/2}\}}{\pi(\phi_i)(1-\phi_i^2)^{1/2}\{|\mu_i| + K_i\sigma_{i\eta}/(1-\phi_i^{*2})^{1/2}\}}\right\}.$$

Third, the conditional posterior density of $\sigma_{i\eta}^{-2}$ is

$$p(\sigma_{i\eta}^{-2}|\mu_i, \phi_i, \beta_{i,1:T}, d_i) \propto TG_{F_i}(\sigma_{i\eta}^{-2}|\hat{v}_i/2, \hat{V}_i/2)\{|\mu_i| + K_i\sigma_{i\eta}/(1-\phi_i^2)^{1/2}\}^{-1},$$

where TG_{F_i} is the density of the implied gamma distribution truncated to $F_i = \{\sigma_{i\eta}^{-2} : d_i < |\mu_i| + K_i\sigma_{i\eta}/(1-\phi_i^2)^{1/2}\}$, and

$$\hat{v}_i = v_{0i} + T, \quad \hat{V}_i = V_{0i} + (1-\phi_i^2)\bar{\beta}_{i1}^2 + \sum_{t=1}^{T-1}(\bar{\beta}_{i,t+1} - \phi_i\bar{\beta}_{it})^2.$$

A Metropolis-Hastings step draws a candidate $1/\sigma_{i\eta}^{*2}$ from this truncated gamma, accepting the draw with probability

$$\min\left\{1, \frac{|\mu_i| + K\sigma_{i\eta}/(1-\phi_i^2)^{1/2}}{|\mu_i| + K\sigma^*_{i\eta}/(1-\phi_i^2)^{1/2}}\right\}.$$

Finally, σ is drawn from $\sigma^{-2}|\boldsymbol{\beta}_{1:T}, \boldsymbol{d}, \boldsymbol{y}_{1:T} \sim G(\hat{n}/2, \hat{S}/2)$, where $\hat{n} = n_0 + T$, and $\hat{S} = S_0 + \sum_{t=1}^{T}(y_t - \boldsymbol{x}_t'\boldsymbol{b}_t)^2$.

A.1.2 Sampling $\boldsymbol{\beta}_{1:T}$

Conditional on $(\boldsymbol{\Theta}, \sigma, \boldsymbol{d}, \boldsymbol{y}_{1:T})$, we sample the conditional posterior at time t, $p(\boldsymbol{\beta}_t|\boldsymbol{\beta}_{-t})$, sequentially for $t = 1 : T$ using a Metropolis-Hastings sampler. The MH proposals come from a non-thresholded version of the model specific to each time t, as follows. Fixing $\boldsymbol{s}_t = \boldsymbol{1}$, take proposal distribution $N(\boldsymbol{\beta}_t|\boldsymbol{m}_t, \boldsymbol{M}_t)$ where

$$\begin{aligned}
\boldsymbol{M}_t^{-1} &= \sigma^{-2}\boldsymbol{x}_t\boldsymbol{x}_t' + \boldsymbol{\Sigma}_\eta^{-1}(\boldsymbol{I} + \boldsymbol{\Phi}'\boldsymbol{\Phi}), \\
\boldsymbol{m}_t &= \boldsymbol{M}_t\left[\sigma^{-2}\boldsymbol{x}_t y_t + \boldsymbol{\Sigma}_\eta^{-1}\left\{\boldsymbol{\Phi}(\boldsymbol{\beta}_{t-1} + \boldsymbol{\beta}_{t+1}) + (\boldsymbol{I} - 2\boldsymbol{\Phi} + \boldsymbol{\Phi}'\boldsymbol{\Phi})\boldsymbol{\mu}\right\}\right],
\end{aligned}$$

for $t = 2 : T-1$. For $t = 1$ and $t = T$, a slight modification is required as follows:

$$\begin{aligned}
\boldsymbol{M}_1^{-1} &= \sigma^{-2}\boldsymbol{x}_1\boldsymbol{x}_1' + \boldsymbol{\Sigma}_{\eta 0}^{-1} + \boldsymbol{\Sigma}_{\eta}^{-1}\boldsymbol{\Phi}'\boldsymbol{\Phi}, \\
\boldsymbol{m}_1 &= \boldsymbol{M}_1\left[\sigma^{-2}\boldsymbol{x}_1 y_1 + \boldsymbol{\Sigma}_{\eta 0}^{-1}\boldsymbol{\mu} + \boldsymbol{\Sigma}_{\eta}^{-1}\boldsymbol{\Phi}\left\{\boldsymbol{\beta}_2 - (\boldsymbol{I}-\boldsymbol{\Phi})\boldsymbol{\mu}\right\}\right], \\
\boldsymbol{M}_T^{-1} &= \sigma^{-2}\boldsymbol{x}_T\boldsymbol{x}_T' + \boldsymbol{\Sigma}_{\eta}^{-1}, \\
\boldsymbol{m}_T &= \boldsymbol{M}_T\left[\sigma^{-2}\boldsymbol{x}_T y_T + \boldsymbol{\Sigma}_{\eta}^{-1}\left\{\boldsymbol{\Phi}\boldsymbol{\beta}_{T-1} + (\boldsymbol{I}-\boldsymbol{\Phi})\boldsymbol{\mu}\right\}\right],
\end{aligned}$$

where $\boldsymbol{\Sigma}_{\eta 0} = \mathrm{diag}(v_1^2, \ldots, v_k^2)$. The candidate is accepted with probability

$$\alpha(\boldsymbol{\beta}_t, \boldsymbol{\beta}_t^*) \;=\; \min\left\{1,\; \frac{N(y_t|\boldsymbol{x}_t'\boldsymbol{b}_t^*, \sigma^2)N(\boldsymbol{\beta}_t|\boldsymbol{m}_t, \boldsymbol{M}_t)}{N(y_t|\boldsymbol{x}_t'\boldsymbol{b}_t, \sigma^2)N(\boldsymbol{\beta}_t^*|\boldsymbol{m}_t, \boldsymbol{M}_t)}\right\},$$

where $\boldsymbol{b}_t = \boldsymbol{\beta}_t \circ \boldsymbol{s}_t$ is the current LTM state at t and $\boldsymbol{b}_t^* = \boldsymbol{\beta}_t^* \circ \boldsymbol{s}_t^*$ the candidate.

A.1.3 Sampling $\boldsymbol{d}$

We adopt a direct MH algorithm to sample the conditional posterior distribution of d_i, conditional on $(\boldsymbol{\Theta}, \sigma, \boldsymbol{\beta}_{1:T}, \boldsymbol{d}_{-i}, \boldsymbol{y}_{1:T})$ where $\boldsymbol{d}_{-i} = d_{1:k}\backslash d_i$. A candidate is drawn from the current conditional prior, $d_i^* \sim U(0, |\mu_i| + K_i v_i)$, and accepted with probability

$$\alpha(d_i, d_i^*) \;=\; \min\left\{1,\; \prod_{t=1}^{T}\frac{N(y_t|\boldsymbol{x}_t'\boldsymbol{b}_t^*, \sigma^2)}{N(y_t|\boldsymbol{x}_t'\boldsymbol{b}_t, \sigma^2)}\right\},$$

where $\boldsymbol{b}_t$ is the state based on the current thresholds $(d_i, \boldsymbol{d}_{-i})$, and $\boldsymbol{b}_t^*$ the candidate based on $(d_i^*, \boldsymbol{d}_{-i})$.

A.2 LT-VAR model

We detail sampling steps for posterior computations in the LT-VAR model where both the VAR coefficients and covariance components of Cholesky-decomposed variance matrices follow LT-AR(1) processes; see eqns. (6)-(7), and (9)-(12). Let $\boldsymbol{\Theta}_{\boldsymbol{\gamma}} = (\boldsymbol{\mu}_{\boldsymbol{\gamma}}, \boldsymbol{\Phi}_{\boldsymbol{\gamma}}, \boldsymbol{V}_{\boldsymbol{\gamma}})$ where $\gamma \in \{\boldsymbol{\beta}, \boldsymbol{\alpha}, \boldsymbol{h}\}$. Standard MCMC algorithms for TV-VAR models are well documented; see, for example, Primiceri (2005), Koop and Korobilis (2010), and Nakajima (2011). These form a basis for the new MCMC sampler in our latent thresholded model extensions.

1. Sampling $\boldsymbol{\beta}_{1:T}$
   Conditional on $(\boldsymbol{\Theta}_{\boldsymbol{\beta}}, \boldsymbol{d}, \boldsymbol{\alpha}_{1:T}, \boldsymbol{h}_{1:T}, \boldsymbol{y}_{1:T})$, $\boldsymbol{\beta}_t$ is generated using the MH sampler implemented in Section . Note that the response here is multivariate; the ingredients in the proposal

distribution are generalized to

$$\begin{aligned}
\boldsymbol{M}_t^{-1} &= \boldsymbol{X}_t'\boldsymbol{\Sigma}_t^{-1}\boldsymbol{X}_t + \boldsymbol{V}_{\boldsymbol{\beta}}^{-1}(\boldsymbol{I} + \boldsymbol{\Phi}'\boldsymbol{\Phi}), \\
\boldsymbol{m}_t &= \boldsymbol{M}_t\left[\boldsymbol{X}_t'\boldsymbol{\Sigma}_t^{-1}\boldsymbol{y}_t + \boldsymbol{V}_{\boldsymbol{\beta}}^{-1}\left\{\boldsymbol{\Phi}(\boldsymbol{\beta}_{t-1} + \boldsymbol{\beta}_{t+1}) + (\boldsymbol{I} - 2\boldsymbol{\Phi} + \boldsymbol{\Phi}'\boldsymbol{\Phi})\boldsymbol{\mu}\right\}\right],
\end{aligned}$$

and the MH acceptance probability is

$$\alpha(\boldsymbol{\beta}_t, \boldsymbol{\beta}_t^*) = \min\left\{1, \frac{N(\boldsymbol{y}_t|\boldsymbol{X}_t\boldsymbol{b}_t^*, \boldsymbol{\Sigma}_t)N(\boldsymbol{\beta}_t|\boldsymbol{m}_t, \boldsymbol{M}_t)}{N(\boldsymbol{y}_t|\boldsymbol{X}_t\boldsymbol{b}_t, \boldsymbol{\Sigma}_t)N(\boldsymbol{\beta}_t^*|\boldsymbol{m}_t, \boldsymbol{M}_t)}\right\}.$$

2. Sampling $\boldsymbol{\alpha}_{1:T}$

   Conditional on $(\boldsymbol{\Theta}_{\boldsymbol{\alpha}}, \boldsymbol{d}_a, \boldsymbol{\beta}_{1:T}, \boldsymbol{h}_{1:T}, \boldsymbol{y}_{1:T})$ where $\boldsymbol{d}_a = \{d_{aij}\}$, sampling $\boldsymbol{\alpha}_{1:T}$ requires the same MH sampling strategy as $\boldsymbol{\beta}_{1:T}$ based on the model (10)-(12).

3. Sampling $\boldsymbol{h}_{1:T}$

   Conditional on $(\boldsymbol{\Theta}_{\boldsymbol{h}}, \boldsymbol{\beta}_{1:T}, \boldsymbol{\alpha}_{1:T}, \boldsymbol{y}_{1:T})$, defining $\boldsymbol{y}_t^* = \boldsymbol{A}_t(\boldsymbol{y}_t - \boldsymbol{X}_t\boldsymbol{\beta}_t)$ and $\boldsymbol{y}_t^* = (y_{1t}^*, \ldots, y_{mt}^*)'$ yields a form of univariate stochastic volatility:

$$\begin{aligned}
y_{it}^* &= \exp(h_{it}/2)e_{it}, \\
h_{it} &= \mu_{hi} + \phi_{hi}(h_{i,t-1} - \mu_{hi}) + \eta_{hit}, \\
(e_{it}, \eta_{hit})' &\sim N\left(\boldsymbol{0}, \mathrm{diag}(1, v_{hi}^2)\right),
\end{aligned}$$

   where μ_{hi}, ϕ_{hi} and v_{hi}^2 are the i-th (diagonal) element of $\boldsymbol{\mu}_{\boldsymbol{h}}, \boldsymbol{\Phi}_{\boldsymbol{h}}$ and $\boldsymbol{V}_{\boldsymbol{h}}$, respectively. As in Primiceri (2005) and Nakajima (2011), we can adopt the standard, efficient algorithm for stochastic volatility models (e.g., Kim et al. (1998), Omori et al. (2007), Shephard and Pitt (1997), Watanabe and Omori (2004)) for this step.

4. Sampling $(\boldsymbol{\Theta}_{\boldsymbol{\beta}}, \boldsymbol{\Theta}_{\boldsymbol{\alpha}}, \boldsymbol{\Theta}_{\boldsymbol{h}})$

   Conditional on $(\boldsymbol{\beta}_{1:T}, \boldsymbol{d})$ and $(\boldsymbol{\alpha}_{1:T}, \boldsymbol{d}_a)$, sampling $\boldsymbol{\Theta}_{\boldsymbol{\beta}}$ and $\boldsymbol{\Theta}_{\boldsymbol{\alpha}}$, respectively, is implemented as in Section . Conditional on $\boldsymbol{h}_{1:T}$, sampling $\boldsymbol{\Theta}_{\boldsymbol{h}}$ also follows the same sampling strategy, although it does not require the rejection step associated with the thresholds.

5. Sampling $(\boldsymbol{d}, \boldsymbol{d}_a)$

   Conditional on all other parameters, we generate the latent thresholds $\boldsymbol{d}$ and $\boldsymbol{d}_a$ using the sampler described in Section .

B Empirical evaluation of MCMC sampling

This appendix reports performance of the MCMC sampler for the LTM in the simulation example. Figure 10 plots autocorrelations and sample paths of MCMC draw for selected parameters of the simulation example (Section 3). In spite of non-linearity of the model structure, the autocorrelations decay quickly and sample paths appear to be stable, indicating the chain mixes well. In addition, MH acceptance rates are empirically high: about 80% for the generation of $\boldsymbol{\beta}_t$ and $\boldsymbol{\alpha}_t$, about 40% for $\boldsymbol{d}$ and $\boldsymbol{d}_a$, and about 95% for $(\boldsymbol{\Theta}_{\boldsymbol{\beta}}, \boldsymbol{\Theta}_{\boldsymbol{\alpha}})$ in the application to macroeconomic data.

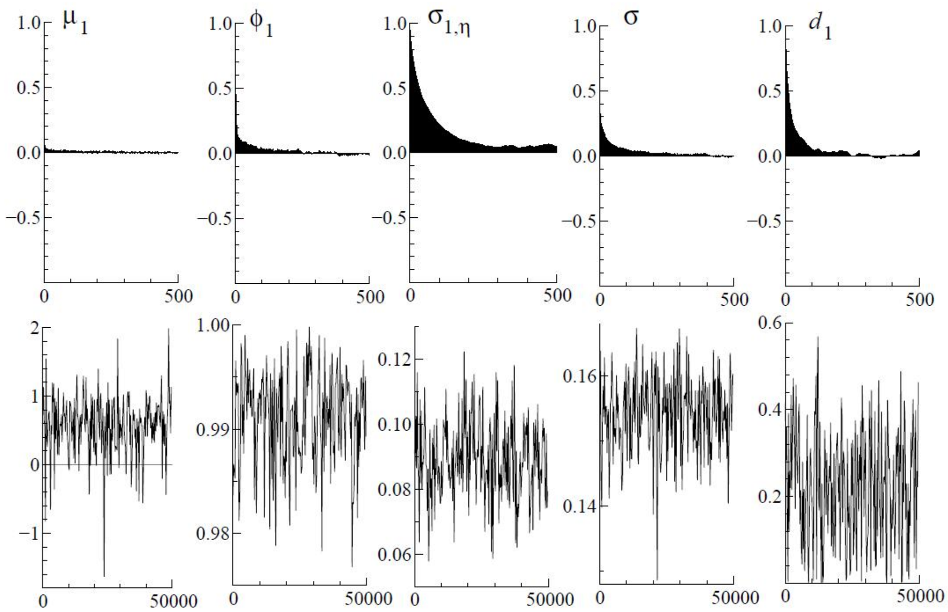

Figure 10: Performance of the MCMC: Autocorrelations (top) and sample paths (bottom) of MCMC draws for selected parameters in simulation example.

To check convergence of MCMC draws, the convergence diagnostic (CD) and relative numerical efficiency measure (a.k.a., effective sample size) of Geweke (1992) are computed. Table 3 reports the CDs (p-values for null hypothesis that the Markov chain converges) as well as inefficiency factors (IFs) for the selected parameters. The CDs indicate the convergence of the MCMC run and the effective sample size is fairy small relative to standard non-linear dynamic models.

	CD	IF
μ_1	0.326	5.0
ϕ_1	0.582	22.1
$\sigma_{1,\eta}$	0.378	107.2
σ	0.150	26.6
d_1	0.503	52.1

Table 3: MCMC diagnostics: Convergence diagnostic (CD) of Geweke (1992) (p-value) and inefficiency factor (IF) for selected parameters in simulation example.

C Additional assessment summaries for US macroeconomic study

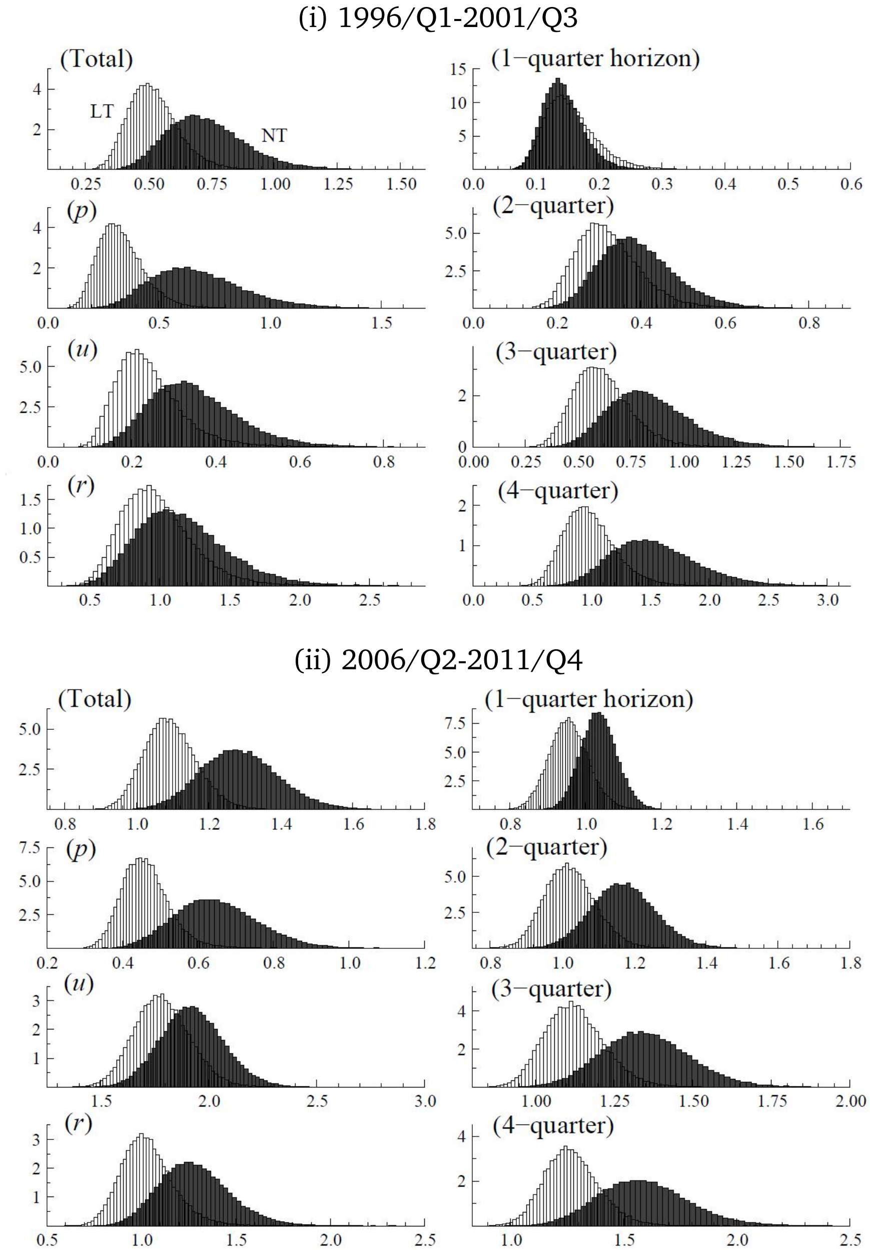

Figure 11: Posteriors of RMSFE from MCMC analysis of US macroeconomic data: (i) 1996/Q1-2001/Q3 and (ii) 2006/Q2-2011/Q4, using NT-VAR (black) and LT-VAR (light) models. Plots are by variable averaged across forecast horizons (left) and by horizon averaged across variables (right). Note the uniform improvements under the LT structure, increased improvements as forecast horizon increases, and increased ability of the LT-VAR models to maintain improved predictive ability in the more volatile second period (ii). Details of RMSFE by variable and horizon, across the full period of recursive out-of-sample forecasting from 2001–2011, are in Table 2.

D Application to Japanese macroeconomic data

D.1 Data

We analyze the $m = 3$ time series giving the quarterly inflation rate, national output gap and short-term interest rate gap in the Japanese economy during 1977/Q1–2007/Q4, following previous analyses of related time series data (Nakajima et al. 2010; Nakajima 2011); see Figure 12. The inflation rate gap is the log-difference from the previous year of the Consumer Price Index (CPI), excluding volatile components of perishable goods and adjusted for nominal impacts of changes in consumption taxes. The output gap is computed as deviations of real from nominal GDP, defined and provided by the Bank of Japan (BOJ). The interest rate gap is computed as log-deviation of the overnight call rate from its HP-filtered trend. One key and evident feature is that the interest rate gap stays at zero during 1999-2000, fixed by the BOJ zero interest rate policy, and again in 2001–2006 when the BOJ introduced a quantitative easing policy. Iwata and Wu (2006) proposed a constant parameter VAR model with a Tobit-type censored variable to estimate monetary policy effects including the zero interest rate periods. In contrast to that customized model, the LTM structure here offers a global, flexible framework to detecting and adapting to underlying structural changes induced by economic and policy activity, including such zero-value data periods. We take the same priors as previous analyses.

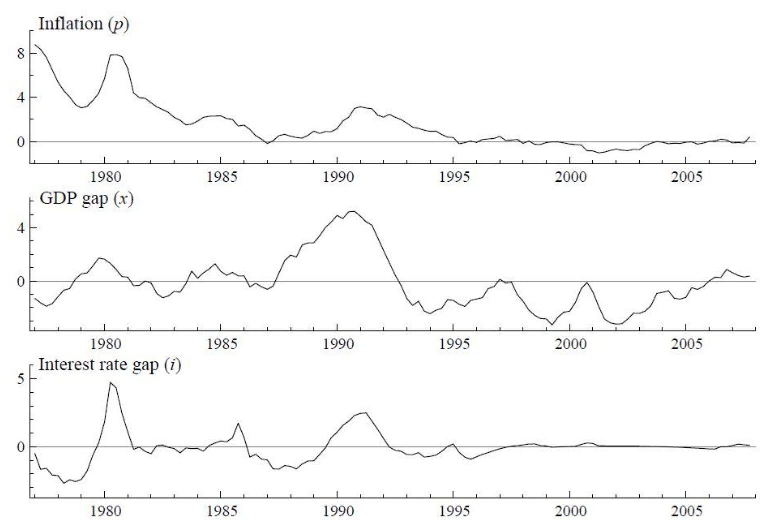

Figure 12: Japanese macroeconomic time series (indices $\times 100$ for % basis).

D.2 Forecasting performance and comparisons

We fit and compare predictions from the NT-VAR and LT-VAR models, as in the study of the US time series. Based on evaluation of RMSFE across the out-of-sample forecasts for the final 4 quarters, it is clear that the LT-VAR models perform best when $p = 2$ is assumed, while the non-threshold TV-VAR models perform best with more elaborate models, taking $p = 4$. The fact that the LTM strategy leads to improved short-term predictions based on reduced dimensional, and hence more parsimonious models is already an indication of the improved fit and statistical efficiency induced by latent thresholding.

		Horizon (quarters)			
		1	2	3	4
RMSFE	NT-VAR	0.253	0.387	0.525	0.633
RMSFE	LT-VAR	0.225	0.263	0.311	0.321
Ratio	LT-VAR/NT-VAR	0.889	0.680	0.592	0.507

Table 4: Forecasting performance for Japanese macroeconomic data: RMSFE for 1- to 4- quarter ahead predictions from NT-VAR and LT-VAR models, averaged over the 3 variables at each horizon.

Some summaries of out-of-sample predictive accuracy appear in Table 4. We computed RMSFE for ten different selections of subsets of data: beginning with the sample period from 1977/Q1–2004/Q3, we fit the model and then forecast 1- to 4-quarters ahead over 2004/Q4–2005/Q3, and then repeat the analysis rolling ahead 1 quarter at a time. Again, the LT-VAR model dominates, improving RMSFE measures quite substantially at all forecast horizons and quite dramatically so at the longer horizons. Improvement relative to the standard NT-VAR are much more distinctive than that of the US macroeconomic data, providing almost half of RMSFE at the 4-quarter horizon. The Japanese data include zero interest rate periods, therefore the benefit from time-varying shrinkage is perhaps expected to be larger than in the US study.

D.3 Some summaries of posterior inferences

Figure 13 displays the posterior means over time of the time-varying coefficients, as well as the posterior probabilities of $s_{it} = 0$ for the LT-VAR model. Some marked patterns of time-varying sparsity are observed for several coefficients. Figure 8 plots the posterior means, the 95% credible intervals of $a_{ij,t}$ and the posterior probabilities of $s_{aij,t} = 0$. Here $a_{21,t}$ has a relatively distinctive shrinkage pattern, with a coefficient that varies slightly and is roughly 50% distinct from zero over most of the time frame, whereas the other two elements – that link directly to the interest rate series – are shrunk to zero with posterior probability close to one across the entire period.

Figure 9 graphs the posterior means of the stochastic volatility, h_{it} and $\exp(h_{it}/2)$, together with their 95% credible intervals. Several volatile periods are observed for the inflation and interest rates series around 1980. It is quite understandable and appropriate that the volatility of the interest rate gap series is estimated close to zero during the zero interest rate periods.

Figure 5 displays posterior means of impulse response for one-, two- and three-year ahead hori-

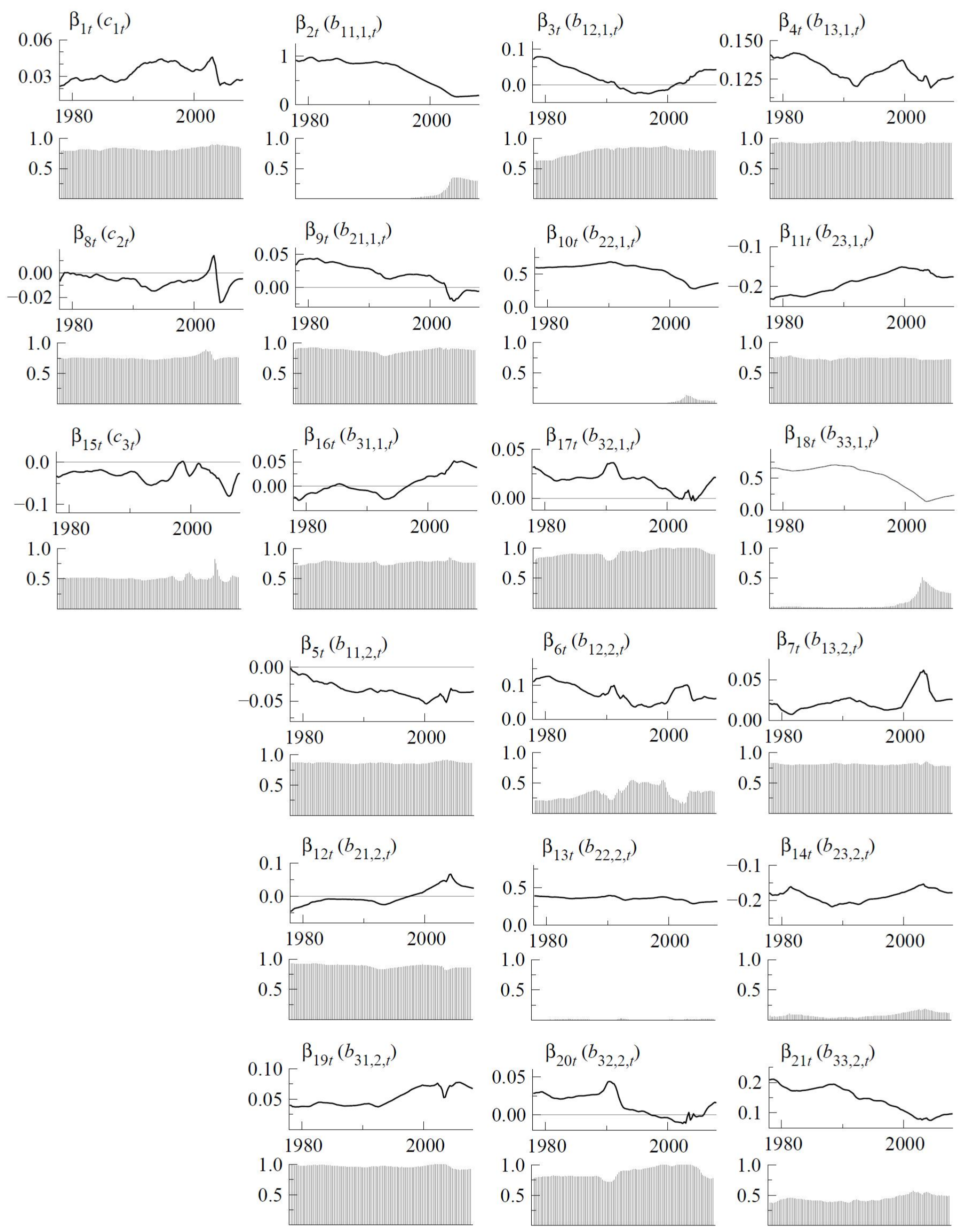

Figure 13: Posterior means of $\boldsymbol{\beta}_t$ for Japanese macroeconomic data. Posterior probabilities of $s_{it} = 0$ are plotted below each trajectory. The corresponding indices of $\boldsymbol{c}_t$ or $\boldsymbol{B}_{\ell t}$ are in parentheses.

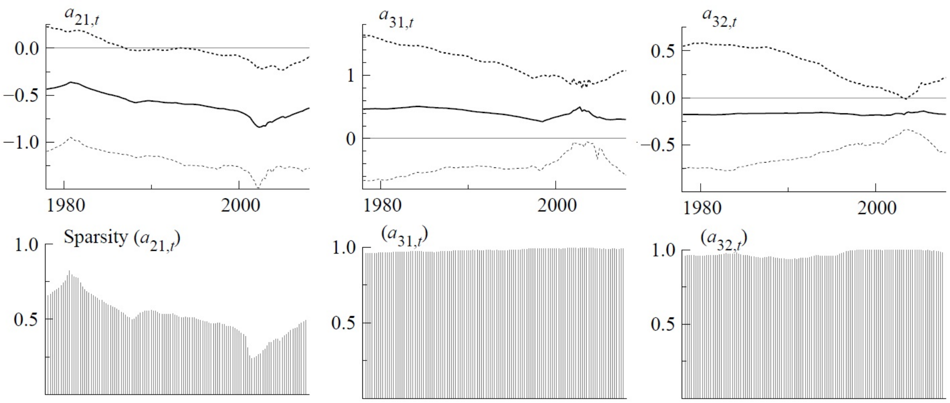

Figure 14: Posterior trajectories of $a_{ij,t}$ for Japanese macroeconomic data: posterior means (solid) and 95% credible intervals (dotted) in the top panels, with posterior probabilities of $s_{aij,t} = 0$ below.

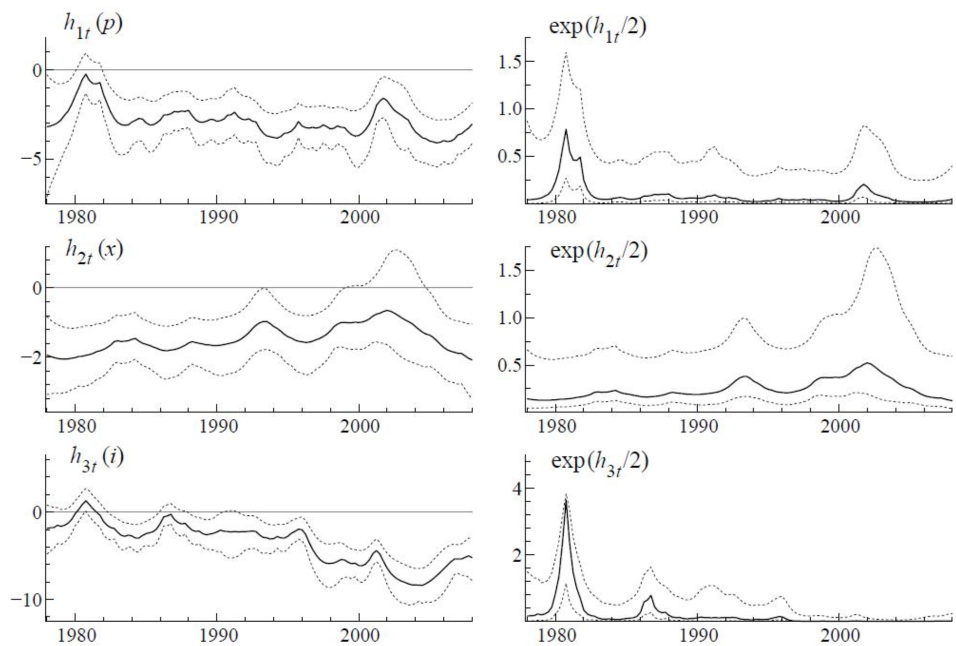

Figure 15: Posterior trajectories of h_{it} and $\exp(h_{it}/2)$ for Japanese macroeconomic data: posterior means (solid) and 95% credible intervals (dotted).

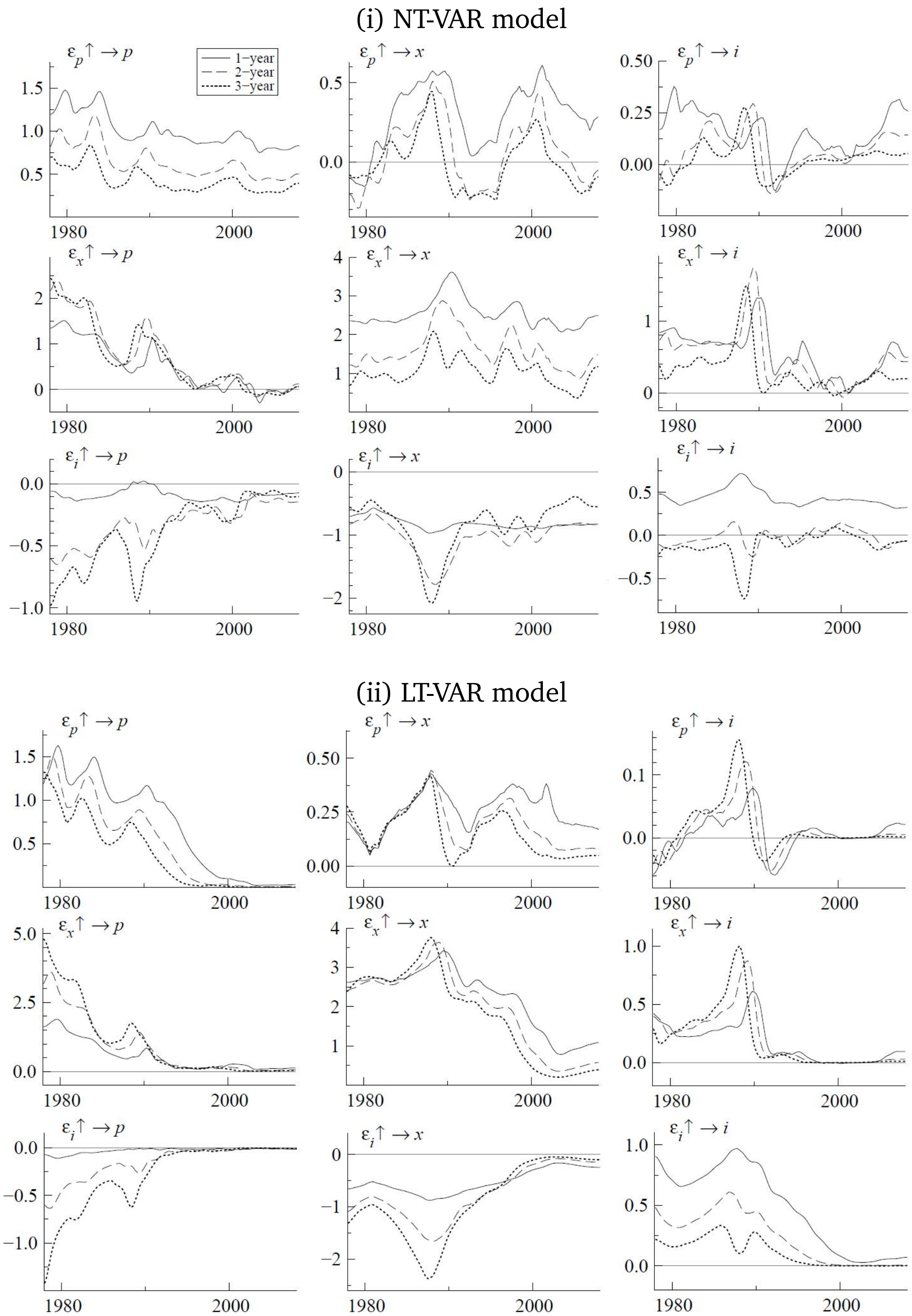

Figure 16: Impulse response trajectories for one-, two- and three-year ahead horizons from the VAR model (upper) and LT-VAR model (lower) for Japanese macroeconomic data. The symbols $\varepsilon_a\!\uparrow\,\to b$ refer to the response of the variable b to a shock to the innovation of variable a. The shock size is set equal to the average of the stochastic volatility across time for each series.

zons. In this comparison, we fitted both the NT-VAR model and the LT-VAR using $p = 2$ lags. The LT-VAR model provides econometrically reasonable responses: the responses of inflation and output to an interest rate shock shrinks to zero during the zero interest rate periods for all horizons. This is not obtained from the NT-VAR model; there the associated time-varying coefficients and covariance components are fluctuating in non-zero values. The responses from the LT-VAR model indicate that the reactions of short-term interest rates to inflation and output decay after the beginning of the 1990s, and afterwards stay at zero due to the zero interest rates. Since the BOJ terminated the quantitative easing policy in 2006, small responses of interest rates are estimated after 2006. The LT-VAR model also suggests that the responses of inflation decay more dramatically to zero in the 1990's than the VAR model indicates. The responses of output to interest rates and to output itself decline more clearly in the LT-VAR model than in the VAR model. These differences obviously result from the LTM structure, which provides these plausible implications for the Japanese macroeconomic analysis as well as the improved multi-step-ahead predictions already discussed.

In addition, Figure 17 reports impulse response with credible intervals computed from posterior draws from NT-VAR and LT-VAR models. Trajectories of posterior median and 75% credible intervals are plotted for responses of the interest rate and inflation to a GDP shock. In both responses, the credible intervals from the LT-VAR model are narrower than that from the NT-VAR and theirs spread is more time-varying; the advantage of LTM structure is obvious particularly in the zero interest rate periods. In addition to the improvements in forecasting performance, these findings confirm that the posterior outputs from the LT-VAR provides more plausible evidences for the macroeconomic dynamics.

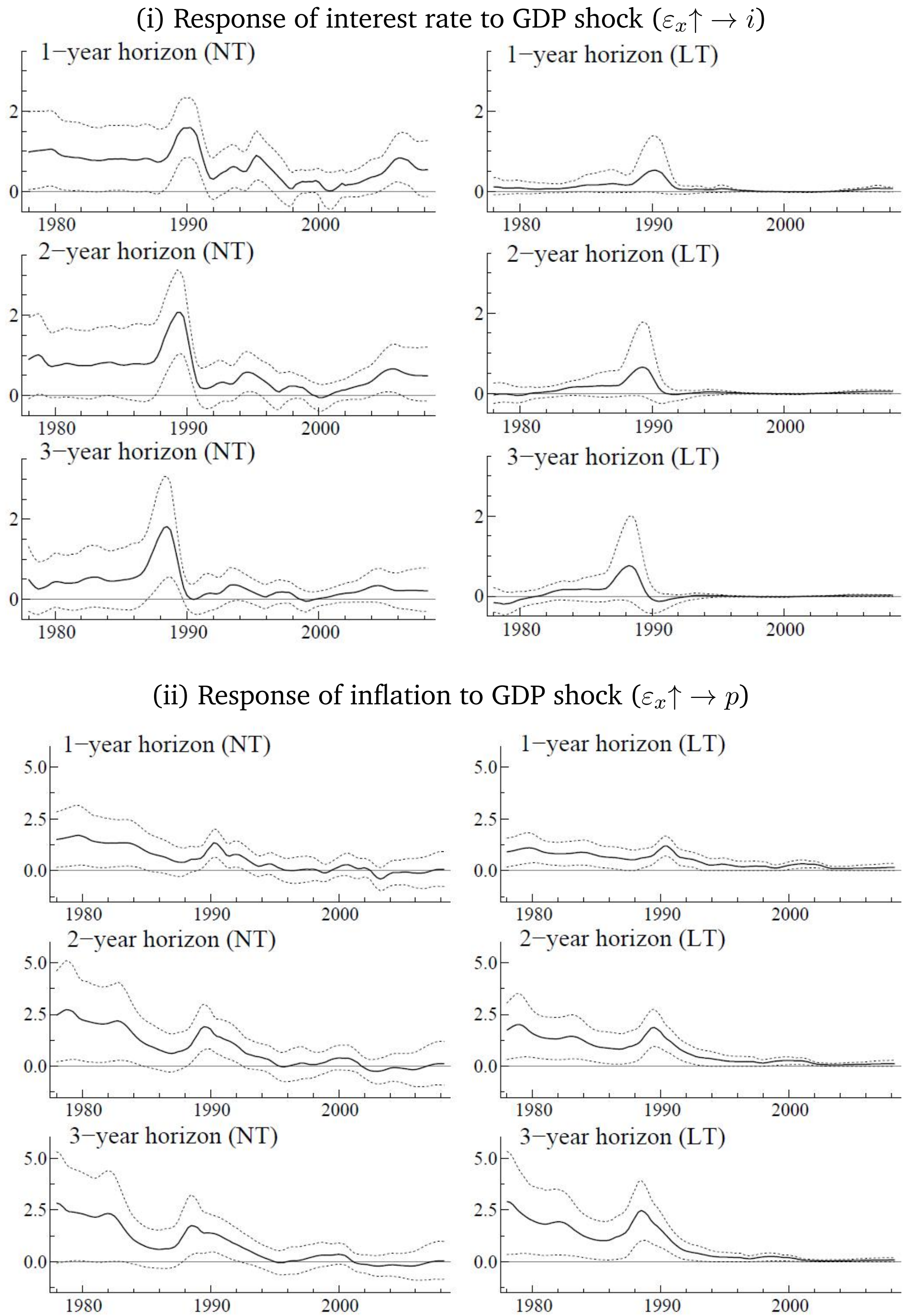

Figure 17: Impulse response trajectories with credible intervals from the NT-VAR (left) and LT-VAR (right) models for Japanese macroeconomic data. Posterior median (solid) and 75% credible intervals (dotted).

References

Geweke, J. (1992), "Evaluating the accuracy of sampling-based approaches to the calculation of posterior moments," in *Bayesian Statistics*, eds. Bernardo, J. M., Berger, J. O., Dawid, A. P., and Smith, A. F. M., New York: Oxford University Press, vol. 4, pp. 169–188.

Iwata, S. and Wu, S. (2006), "Estimating monetary policy effects when interest rates are close to zero," *Journal of Monetary Economics*, 53, 1395–1408.

Kim, S., Shephard, N., and Chib, S. (1998), "Stochastic volatility: likelihood inference and comparison with ARCH models," *Review of Economic Studies*, 65, 361–393.

Koop, G. and Korobilis, D. (2010), "Bayesian multivariate time series methods for empirical macroeconomics," *Foundations and Trends in Econometrics*, 3, 267–358.

Nakajima, J. (2011), "Time-varying parameter VAR model with stochastic volatility: An overview of methodology and empirical applications," *Monetary and Economic Studies*, 29, 107–142.

Nakajima, J., Shiratsuka, S., and Teranishi, Y. (2010), "The effects of monetary policy commitment: Evidence from time-varying parameter VAR analysis," IMES Discussion Paper, 2010-E-6, Bank of Japan.

Omori, Y., Chib, S., Shephard, N., and Nakajima, J. (2007), "Stochastic volatility with leverage: Fast likelihood inference," *Journal of Econometrics*, 140, 425–449.

Primiceri, G. E. (2005), "Time varying structural vector autoregressions and monetary policy," *Review of Economic Studies*, 72, 821–852.

Shephard, N. and Pitt, M. (1997), "Likelihood analysis of non-Gaussian measurement time series," *Biometrika*, 84, 653–667.

Watanabe, T. and Omori, Y. (2004), "A multi-move sampler for estimating non-Gaussian time series models: Comments on Shephard and Pitt (1997)," *Biometrika*, 91, 246–248.